Received: 19 September 2018 | Revised: 12 November 2018 | Accepted: 20 November 2018

DOI: 10.1002/aoc.4765

WILEY Applied Organometallic Chemistry

FULL PAPER

The functionality of the hybrid systems driven by molecular dimension of the guest copper Schiff-base complexes entrapped in Zeolite-Y

Susheela Kumari | Archana Choudhary | Saumi Ray

Birla Institute of Technology and Science, Pilani, Rajasthan 333031, India

Correspondence
Saumi Ray, Department of Chemistry, Birla Institute of Technology and Science, Pilani, Rajasthan 333031 India.
Email: saumi@pilani.bits-pilani.ac.in

On encapsulation inside the supercage of zeolite-Y planar Cu (II)–Schiff base complexes show the modified structural, optical and functional properties. The electronic effect of the different substituent groups present in the catalyst plays the decisive role towards their reactivity in the homogeneous phase but after the encapsulation in zeolite Y, reactivity is mainly governed by the molecular dimensions of the guest complexes rather than the electronic factor of the substituent groups attached on them. These systems are well characterized with the help of different characterization tools like XRD analysis, SEM - EDX, AAS, FTIR, XPS, DSC, TGA, BET and UV–Visible spectroscopy and the comparative optical and catalytic studies have provided a rational explanation of enhanced reactivity of zeolite encapsulated metal complexes for various oxidation reactions compared to their corresponding solution states.

KEYWORDS
catalysis, copper Schiff-base complexes, encapsulation, styrene oxidation, zeolite-Y

1 | INTRODUCTION

Transformation of hydrocarbons into their oxy-functionalized derivatives are the important chemical processes for the industrial and academic purpose. Transition metal complexes are usually efficient catalysts for the oxidation of various organic compounds in mild reaction conditions; however, these homogeneous catalysts always have some drawbacks in the catalytic process like their instability, difficulty in the separation, and lack of reusability.[1,2]

The state-of-the-art of the catalytic science prefers such type of catalysts, which can overcome the limitations of the homogeneous catalytic processes without the loss of reactivity. In this direction heterogenization of the homogeneous catalyst is a convenient approach to couple the reactivity of the complex with the stability, specific environment and ease of separation provided by host materials. Impregnation and encapsulation of transition metal complexes in the microporous,[3–6] mesoporous materials[7] and MOFs,[8,9] homogeneous catalyst tagged with ionic liquids,[10,11] alumina-supported metal complexes[12] and phase transfer catalyst[13] are some interesting examples of heterogeneous systems, which have been successfully employed in the various oxidation reactions by using H_2O_2, TBHP, and molecular O_2 as oxidants.[14,15] Zeolites, the microporous aluminosilicate materials are the competent hosts for the encapsulation of transition metal complexes having the molecular dimension comparable with the diameter cavities of the host zeolites.[5,16] These contemporary classes of catalysts comprise the catalyst molecule encapsulated within the well-structured architecture of the host, with a large surface area. This is undoubtedly a unique way of site isolation of the desired catalyst. These systems have shown a structural and functional analogy with cytochrome P450,[17] and are well explored as the proficient catalysts for the selective oxidative transformation of olefinic C-H

bonds to its oxy-derivatives. P. Ratanasmy *et al*. have reported that both copper salen and 5-chloro copper salen complexes, when encapsulated in zeolite Y suffer from structural distortion and also are recognized as efficient catalysts for the oxidation of p-xylene and phenol. The authors also emphasize upon the fact that the presence of electron withdrawing group on the phenyl rings immensely improves the TOF, h^{-1} of the oxidation reaction.[2]

Few more reports are available in the literature, which also recognize the distorted geometry of the guest complex under space constraint imposed by the zeolite framework is the primary reason for enhanced reactivity of the encapsulated complex. Maurya M. R. *et al*. have studied catalytic activities of different metal complexes encapsulated in zeolite Y for oxidation of different hydrocarbons such as styrene, cyclohexane, cyclohexene, and methyl phenyl sulfide, where authors have evidently shown that encapsulated complexes are much more reactive for oxidative transformation than the corresponding free state complex.[3,14,18,19] Some other reports on the encapsulated metal phthalocyanine and Tris(2,2′ bipyridine) iron complexes for the oxidation reaction for phenols, styrene, and methyl styrene also confirm that the free state complex especially Tris(2,2bipyridine) iron complex is definitely not so efficient catalyst like its encapsulated analogue in identical reaction conditions.[20] Recently, R. Ananthakrishnan and coworkers have reported the synthesis of $[Ru(bpy)_3]Cl_2$ complex on a mesoporous silica SBA-15 support and its application for degradation of chlorophenol under visible light in an aqueous medium.[21] In another report, an encapsulated chiral nickel Schiff base complexes inside the cavity of zeolite Y has been recognized as an excellent catalyst for asymmetric Henry reaction.[22] In another comparative study of different metal picolinato complexes in zeolite Y, R. C. Deka *et al*. have observed that the copper and cobalt complexes are more reactive catalysts compared to the its corresponding nickel complexes for the selective oxidation of phenol by using H_2O_2 as the oxidant.[6] It is quite clear that the encapsulated complexes in zeolite Y are competent catalysts for oxidation of hydrocarbons, and most of the studies have suggested that enhanced activity of the encapsulated complex is definitely a consequence of the distorted geometry of the complex under space constraint inside the rigid cavity.[23,24] Already the diverse effects of different substituents on the structure and functionality of the copper Schiff-base complexes are discussed thoroughly.[25] Bhadbhade *et al*. have explored the effect of substituents (H, $-OCH_3$ and -Cl on Cu-salen, 5-OCH_3-Cu-salen, and 5-chloro-Cu-salen) on various aspects like molecular association, conformation, and electronic structure. Cu-salen complex forms strong dimers and stepped confirmation and 5-OCH_3-Cu-salen complex, which has an electron-donating $-OCH_3$ substituent maintains more planarity around the metal center proximity and forms weak dimer whereas an electron withdrawing chloro-substituted complex (5-chloro-Cu-salen) is essentially a monomer in solid state and have distorted square-planar geometry around CuN_2O_2 proximity.[25] It is interesting to know the diverse effects of molecular association e.g., steric and electronic effects and ligand architecture on the reactivity of the catalyst in the homogeneous and heterogeneous states.

In the present study, we choose the complexes with different substitution (H, OH, Br and - OCH_3 on the 5th position of the phenyl rings) on the phenyl rings of Schiff base salen and salophen ligands. These complexes of two different series copper salen and copper salophen are abbreviated as CuS1, CuS2, CuS3 and CuS4 and CuSp1, CuSp2, CuSp3 and CuSp4 respectively. In a particular series, complexes (say, from CuS1 to CuS4) vary on the basis of their increasing order of the molecular dimensions and these are encapsulated inside nearly spherical supercage of zeolite Y via flexible ligand synthesis method (given in scheme 1). These systems are well characterized with the help of powdered XRD, AAS, SEM-EDS, IR, XPS, DSC, TGA, BET and UV–Visible spectroscopy. We employ the systems as catalysts for the styrene oxidation reaction.

The encapsulation and catalysis of different copper complexes in the voids of zeolite Y are extensively studied;[26] however, the systematic approach to study the structural changes of the complexes upon encapsulation are still on demand. Our selection of the copper Schiff-base complexes largely depends upon the end-to-end distance of the complex so that the host supercage of 12.47 Å diameter imposes the steric constraints on the guest complex. Under such condition, the geometry adopted by the complex are studied thoroughly. Detailed studies of modified reactivity towards styrene oxidation evolving from structural distortion as a function of the end-to-end distance of the complex is the prime objective of our research.

Comparative structural and catalytic studies of these coupled systems have been carried out in detail to comprehend the geometry of the complex after encapsulation as well as to identify the origin of the modified functionality of the systems. Research on the link between enhanced selective catalysis and adopted geometry of the guest complex is relatively rare in the literature and our research attempts to address this question. Comparative studies reveal quite a fascinating correlation existing between the catalytic activities and modified structure experienced by the complexes under encapsulation which leaves a lot of scopes to further modify the activity of the catalysts and to have a better insight of these heterogeneous systems.

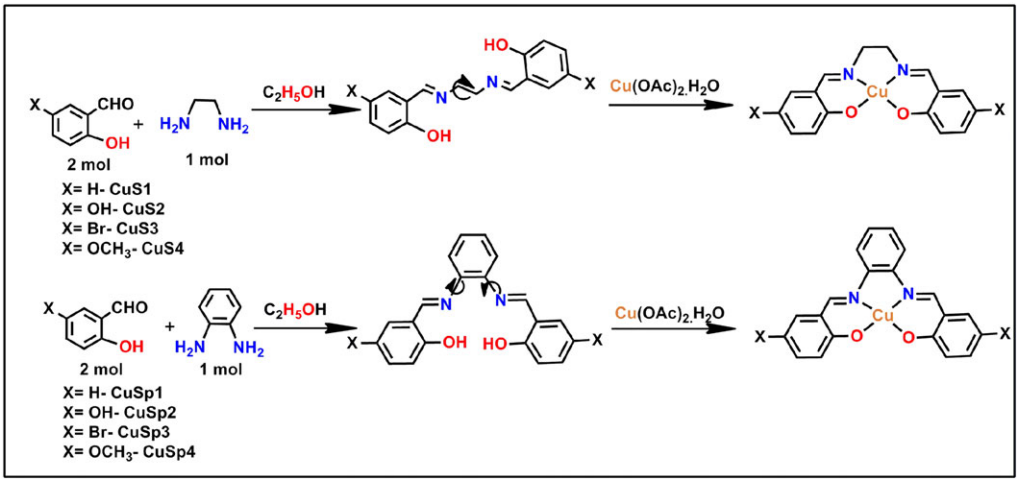

SCHEME 1 Synthesis of copper Schiff-bases complexes derived from ethylene diamine (or 1, 2 diamino benzene) and salicyaldehyde (or its derivetives)

2 | EXPERIMENTAL SECTION

2.1 | Materials and preparation

Pure zeolite-Y was purchased from sigma – Aldrich, Delhi, India. salicylaldehyde and its derivatives, phenyl diamine, ethylene diamine are purchased from alfa aecer and copper acetate and solvents (ethanol, acetone, methanol and diethyl ether) were purchased from S.D. fine, Delhi, India.

2.2 | Preparation of ligand and complexes[2,23]

The salen and the salophen ligand was synthesized as follows. Two mole of salicylaldehyde (or its derivatives) was dissolved in ethanol and refluxed for (10–15) minutes. One mole of ethylene-diamine (or phenylene diamine) was added into it in order to synthesize salen (or salophen) ligands. The reaction mixture was refluxed for (30–120) minutes at (60–70)°C and then ice cooled for 1 hr. A bright yellow solid flakes were obtained as product which was thoroughly washed with ethanol and then dried in air (given in scheme 1).

For the synthesis of free state salen and salophen complexes, the ligands (S1, S2, S3, and S4) and (Sp1, Sp2, Sp3, and Sp4) were dissolved in ethanol and refluxed under N_2 atmosphere. An equi molar ratio of copper acetate solution was added drop-wise into the reaction mixture and further refluxed for the (30–240) minutes for the synthesis of different complexes. The reaction mass was recovered, filtered and washed with ethanol and diethyl ether and then further air dried at room temperature (given in scheme 1).

2.3 | Synthesis of Cu-exchanged zeolite Y and encapsulated of Cu (II) Schiff-base complex[2,27]

Pure Na-zeolite Y ($Na_{58}Al_{58}Si_{136}O_{388}{\bullet}yH_2O$) was dispersed in 0.01 M copper acetate solution and stirred at room temperature for 24 hr to obtain the desired loading level of copper metal ions in the zeolite. The slurry was filtered, washed repeatedly with deionized water and desiccated for 12 hr at 150 °C. Synthesis of copper (II) Schiff base complex was carried out via 'flexible ligand' approach' (given in scheme 2). The Cu-exchanged zeolite and excess amount of ligands were heated together under solvent-free condition at (200–250)°C as the melting points of different ligands vary approximately from 160–230 °C, with constant stirring for 24 hr. To synthesize the complex inside the supercage of zeolite Y, diffusion of melted ligand through zeolite pore is mandatory. On heating, the color of the solid reaction mass was changed from pale yellow to reddish-brown. The solid reaction mixture was recovered and further subjected to Soxhlet extraction with the different solvents maintaining the order, like as acetone, methanol, and finally diethyl ether. The product was dried in a muffle furnace for (10–12) h at 150 °C. The recovered product was further treated with 0.01 M NaCl solution for 12 hr to remove the unreacted Cu^{2+} ions, followed by filtration and continuous washing until the filtrate is free from the chloride ion.

2.4 | Catalytic oxidation reaction

To investigate the catalytic activity of the encapsulated complexes, styrene oxidation transformation catalyzed by copper Schiff-base complexes in free and encapsulated

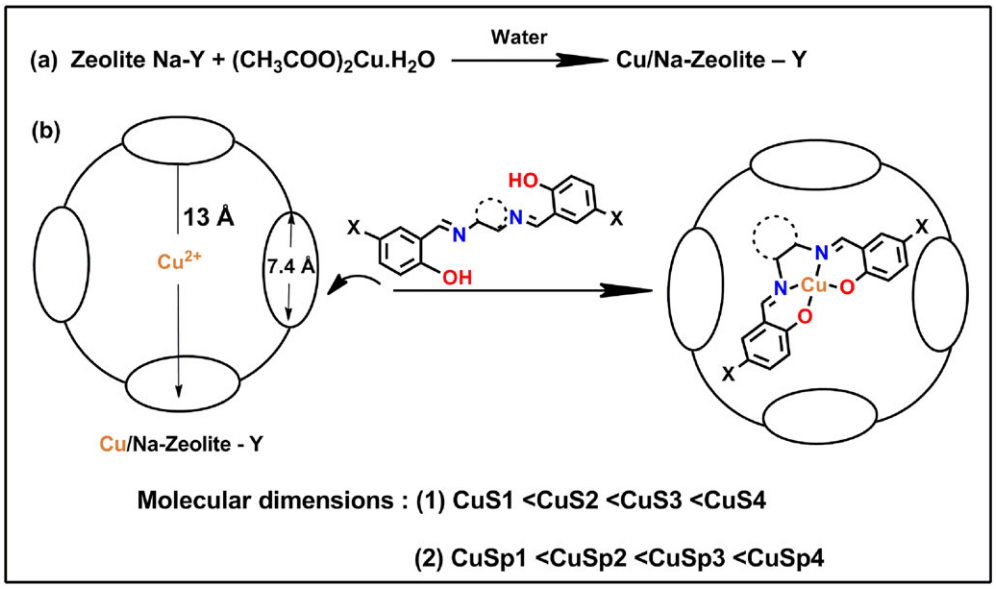

SCHEME 2 Schematic representation of encapsulation of metal complex in the supercage of zeolite via 'flexible ligand method' to prepare 'ship-in-a-bottle' complex

states were explored by using H_2O_2 as an oxidant in the aerobic condition. The optimum conditions for epoxidation reaction were as follows: (Styrene: 1.56 g, 15 mmol), (H_2O_2: 3.40 g, 30 mmol), acetonitrile 15 ml, temperature 80 °C, and catalyst (0.05 g for encapsulated complexes and 0.0045 g for neat complexes). After the reaction was finished, the products were identified and quantified with the help of Gas Chromatography by using the internal standard method.

3 | RESULTS AND DISCUSSIONS

3.1 | Elemental analysis

Parent zeolite has Si/Al ratio of 2.34 and its unit cell formula of the host material is $Na_{58}Al_{58}Si_{136}O_{388}$ yH_2O. The Si/Al ratio of host framework remains unaffected even after the complete synthesis of the metal complex inside it which essentially signifies the lack of dealumination during the whole process of ion exchange and encapsulation (EDX data are given in supporting information Figure S1).[28] The concentration of metals in different samples are determined by atomic absorption spectroscopy and it is found that the metal content in the encapsulated Cu complexes is always less than that present in the Cu- exchanged zeolite Y (AAS data given in Table 1). The observation essentially indicates the complex formation inside the host cavity with slight leaching of some of the metal ions during the process of encapsulation.

3.2 | Catalytic study

Catalytic activities of the metal complexes in their free and encapsulated states are explored by studying the oxidation reaction of styrene and then compared. Styrene can be oxidized into the different organic compounds as benzaldehyde, styrene oxide, benzoic acid, phenylacetaldehyde and phenylethane-1, 2-diol; some of these products of the reaction are previously reported.[3,14] Calibration curve of styrene, benzaldehyde and styrene oxide are shown in supporting information (Figure S2 A-C). Reaction conditions are optimized with respect to the CuS1 complex in the encapsulated state as the representative catalyst by varying different reaction parameters like temperature, the time duration of reaction and amount of catalysts to attain maximum efficiency. To standardize the reaction condition, styrene (1.56 g, 15 mmol) and 30% H_2O_2 (3.40 g, 30 mmol) are mixed with 15 ml acetonitrile and catalysts of different amounts (0.015 g, 0.030 g and 0.05 g) are added at various temperatures 40 °C, 80 °C and 120 °C for variable reaction durations (2 hr, 5 hr and 8 hr). Initially, the amount of catalysts is optimized for encapsulated CuS1 in zeolite Y as it has shown the improved reactivity when employed in two different sets of reaction with 0.030 g and 0.050 g. The conversion of styrene is found to be the least when 0.015 g of the catalyst is used (catalytic data are presented in supporting information, Table S1-S3, and Figure S3). We have considered 0.050 g as an optimized amount of the catalysts for above reaction conditions because no substantial improvement in the % conversion of styrene is observed while taking 0.070 g of the catalysts. A further

TABLE 1 Amount of Cu-atom (mmol) for all catalysts

S. No	Catalyst	Cu-atom in catalyst (mmol)[a]	S. No	Catalyst	% weight of Cu[b]	Cu-atom in catalyst (mmol) [a]
1	**Zeolite-Y**	-	**2**	**Cu-Y**	0.81	0.00637
3	**CuS1**	0.01360	**4**	**CuS1-Y**	0.62	0.00487
5	**CuS2**	0.01240	**6**	**CuS2-Y**	0.59	0.00464
7	**CuS3**	0.00922	**8**	**CuS3-Y**	0.37	0.00291
9	**CuS4**	0.01154	**10**	**CuS4-Y**	0.39	0.00306
11	**CuSp1**	0.01190	**12**	**CuSp1-Y**	0.67	0.00527
13	**CuSp2**	0.01090	**14**	**CuSp2-Y**	0.52	0.00409
15	**CuSp3**	0.00840	**16**	**CuSp3-Y**	0.39	0.00306
17	**CuSp4**	0.01020	**18**	**CuSp4-Y**	0.34	0.00267

[a]mmol of Cu atom calculated in 0.0045 g for neat complexes and 0.05 g for encapsulated complexes and Cu-Y).

[b]% weight of Cu obtained from AAS.

increase in the amount of catalyst causes a drop in % conversion since it lowers the probably of adsorption of two different reactant molecules on the same catalytic site hence reduces the effective interaction between reactant molecules.[3]

For the oxidation reaction, styrene (1.56 g, 15 mmol), 30% H_2O_2 (3.40 g, 30 mmol) in 15 ml acetonitrile and 0.050 g catalyst have been kept for different time durations e.g., 2 hr, 5 hr and 8 hr. Since there is no significant improvement observed in the % conversion of styrene after 8 hr and this is chosen as the adequate time for the reaction. With these optimized conditions, the styrene oxidation reaction is studied at three different temperatures 40 °C, 80 °C and 120 °C, and conversion of styrene is quantified as 5%, 47% and 58% for the encapsulated CuS1 complex at 40 °C, 80 °C and 120 °C, respectively. Therefore, 80 °C temperature is found to be the appropriate/optimum temperature for the reaction. However, for the free state complexes, quite a low amount of 0.0045 g has been employed as a catalyst in each of the cases because within this amount, the neat complexes have active metal centers much higher in number as compared to their analogous encapsulated state complexes. Comparative studies (shown in Table 1) clearly indicate that 0.0045 g free state complex still contains 2–4 times higher the amount of Cu active centers than that present in 0.05 g of the corresponding encapsulated complex. Within the optimum range of the amount of catalyst, more the number of active metal sites more is the % conversion of styrene. Therefore, to study catalysis driven by the geometry of the metal complex, the rationale is to reduce the catalytic data in terms of the turnover number (TON) rather than the % conversion so that difference in concentrations of active metal centers in both the states could be nullified. With these suitable conditions, copper salen complexes (CuS1, CuS2, CuS3, and CuS4) and copper salophen complexes (CuSp1, CuSp2, CuSp3, and CuSp4) are employed as catalysts in free as well as encapsulated states (catalytic data presented in Table 2). These catalysts are more selective for benzaldehyde formation in both states while the other products like styrene oxide are formed as a minor product along with negligibly small amounts of benzoic acid and phenylacetaldehyde as shown in Table 2. The higher yield of benzaldehyde might be associated with the formation of hydroperoxylstyrene intermediate by the nucleophilic attack of H_2O_2, which is further cleaved to produce benzaldehyde. Another route of formation of benzaldehyde is further oxidation of styrene oxide, one of the products of the styrene oxidation. The formation of benzoic acid is the result of further oxidation of benzaldehyde and phenylacetaldehyde is the isomerized product of styrene oxide.[29]

Turn over number (TON) calculated from the catalytic data have repeatedly shown a clear-cut reactivity trend; free state salen and salophen complexes follow the reactivity order as CuS3 > CuS1 > CuS2 > CuS4 and CuSp1 > CuSp3 > CuSp2 > CuSp4 respectively however upon encapsulation within zeolite Y, scenario changes. It is CuS4 > CuS3 > CuS1 > CuS2 for the encapsulated salen complexes, whereas the encapsulated salophen complexes demonstrate the order as CuSp4 > CuSp3 > CuSp2 > CuSp1.The catalytic activity is certainly governed by the electronic factor or electron density on the metal when the complexes are in their free states. Complexes with different substituent groups render electron density of the metal differently, and consequently, the outcome of catalysis varies, however, after encapsulation, the steric constraint imposed by the zeolite framework upon the guest complex contributes significantly to the catalytic activity. On encapsulation, the complexes with larger molecular dimension possibly

TABLE 2 Conversion of styrene after 8 hr reaction time with H_2O_2 as oxidant

S. No	Samples	% Conversion	TON	Selectivity		S. No	Samples	% Conversion	TON	Selectivity	
				Benz.	SO					Benz.	SO
1	**Zeolite-Y**	3	-	73.97	26.02	2	**Cu-Y**	20	455.2	90.90	9.09
3	**CuS1**	86	941.1	81.83	18.16	4	**CuS1-Y**	47	1435.3	96.35	3.64
5	**CuS2**	56	677.4	89.79	10.20	6	**CuS2-Y**	23	711.2	99.30	0.69
7	**CuS3**	76	1236.4	87.80	12.19	8	**CuS3-Y**	54	2793.8	91.64	8.35
9	**CuS4**	50	649.9	90.47	9.52	10	**CuS4-Y**	64	3137.2	96.87	3.12
11	**CuSp1**	74	937.8	89.47	10.52	12	**CuSp1-Y**	50	1423.1	93.15	6.84
13	**CuSp2**	59	807.3	89.62	10.37	14	**CuSp2-Y**	57	2078.2	91.05	8.94
15	**CuSp3**	50	892.8	95.45	4.54	16	**CuSp3-Y**	62	3042.4	97.56	2.43
17	**CuSp4**	12	187.2	93.41	6.59	18	**CuSp4-Y**	63	3543	95.17	4.82

Reaction conditions: Reaction conditions (Styrene: 1.56 g, 15 mmol), (H_2O_2: 3.40 g, 30 mmol), acetonitrile 15 ml, temperature 80 °C, catalyst (0.05 g for encapsulated complexes and 0.0045 g for neat complexes),TON (turn over number): mole of substrate converted per mole of metal center (encapsulated complexes), Benz.: Benzaldehyde, SO: Styrene oxide.

undergo more distortion imposed by the supercage, finally leading to the alteration of the overall reactivity order. Hence, the final structure adopted by the encapsulated complex is the major decisive factor for improved catalysis. Therefore, to understand to verify the mechanism of a catalytic reaction and the appropriate structural involvement of the catalyst, encapsulation could be a technically potent process. Detailed structural analysis of the complex especially after encapsulation inside zeolite is expected to provide the insight of the catalytic process hence, leads to the route of the tunable catalysis. The CuS4-Y catalyst is found to be efficient enough for this oxidation reaction up to six cycles with a marginal loss in its catalytic activity as in form of percentage conversion from 64% to 63.3% (Shown in Figure 1).

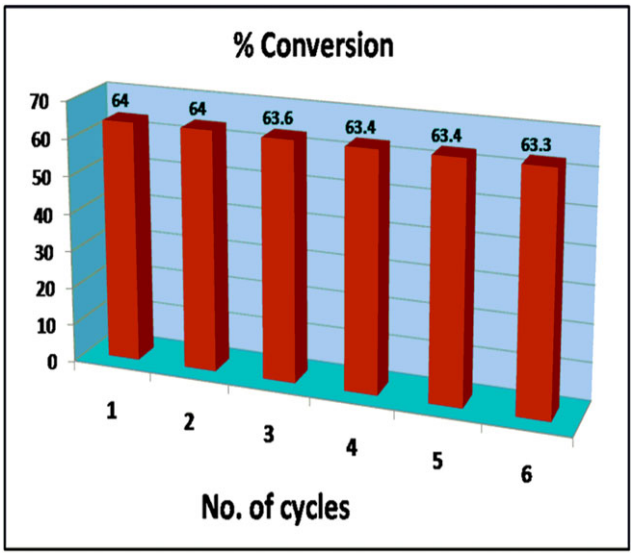

FIGURE 1 Recyclability of the CuS4-Ycatalyst for styrene oxidation reaction

3.3 | X-ray diffraction and scanning electron microscopy analysis

To investigate the order of retention of zeolite crystallinity, surface morphology, and integrity of host zeolite Y, XRD patterns of parent zeolite Y, Cu-zeolite Y and zeolite with encapsulated copper Schiff-base complexes are recorded. (XRD pattern are given in Figure 2) Essentially similar patterns of all the samples indicate the preservation of the integrity of the host framework during the process of encapsulation. On comparison of the XRD patterns of encapsulated complexes with the pure and copper exchanged zeolite-Y, an evident distinction in the XRD patterns of the encapsulated complexes has been observed. Alteration of relative intensities of peaks at the $2\theta = 10°$ and 12° are noticed after encapsulation. For parent zeolite and Cu-exchanged zeolite the relation $I_{220} > I_{311}$ exist, but for zeolite, with encapsulated complexes, the relation is just reverse; $I_{311} > I_{220}$. The observed modification in these intensities after the encapsulation previously has been recognized and empirically associated with the fact that a large complex is indeed present within the zeolite-Y supercage.[30] Scanning electron microscopy also supports the fact that the complex formation is primarily taking place inside the host cavities. From the SEM images (SEM micrographs given in Figure 3a-3c before Soxhlet extraction for CuS4-Y with different resolution; Figure 3d-3f for CuS4-Y and Figure 3g-3i for CuSp4-Y after Soxhlet extraction and Figure S4 in supporting information for CuS1-Y and CuSp1-Y), it is observed that before Soxhlet extraction, there are some detectable surface species probably due to the formation of the complex at the surface or un-reacted ligands, however,

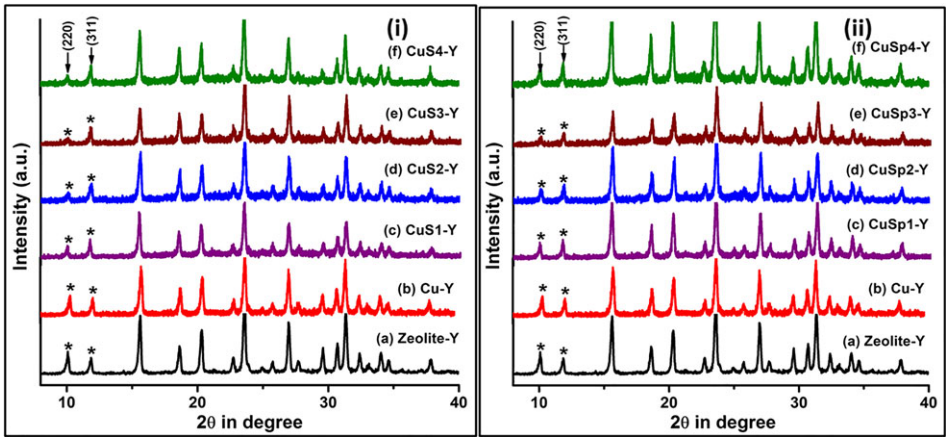

FIGURE 2 (i) Powder XRD patterns of (a) pure zeolite-Y (b) Cu- exchanged zeolite-Y, (c) CuS1-Y, (d) CuS2-Y, (e) CuS3-Y and (f) CuS4-Y. (ii) Powder XRD patterns of (a) pure zeolite-Y, (b) Cu - exchanged zeolite-Y, (c) CuSp1-Y, (d) CuSp2-Y, (e) CuSp3-Y and (f) CuSp4-Y

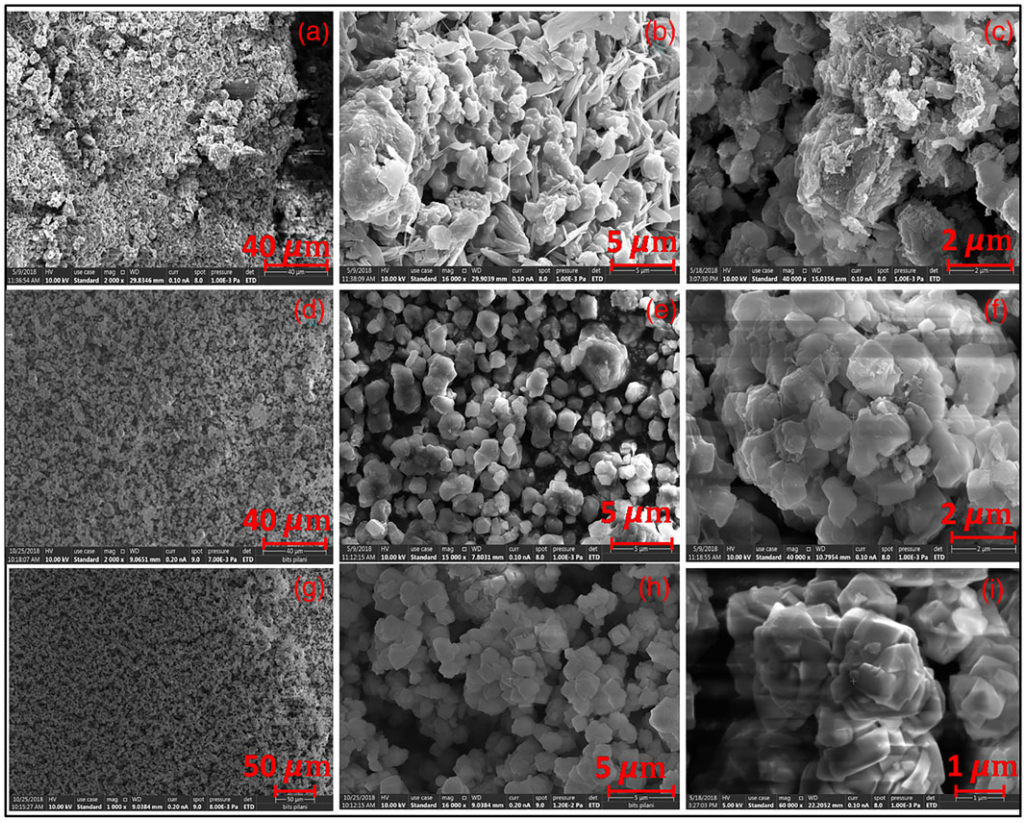

FIGURE 3 SEM images before Soxhlet extraction (a-c) CuS4-Y with different resolution, and after Soxhlet extraction (d-f) CuS4-Yand (g-i) CuSp4-Y

are disappeared after Soxhlet extraction.[28,31] making zeolite particle boundaries more clearly visible. The clarity in the observation of boundaries of host lattice in SEM micrographs and the persistent color of Soxhlet extracted final product are certainly logical indications of successful encapsulation of the complex inside the cavities of zeolite Y.

3.4 | IR spectroscopic study

IR spectral data of ligands, (given in supporting information Figure S5 and Table S5) pure zeolite Y and all copper Schiff-base complexes in free and encapsulated states are given in Figure 4 and Table S4. Pure zeolite Y has shown strong IR peak at 1018 cm^{-1}, which is mainly attributed

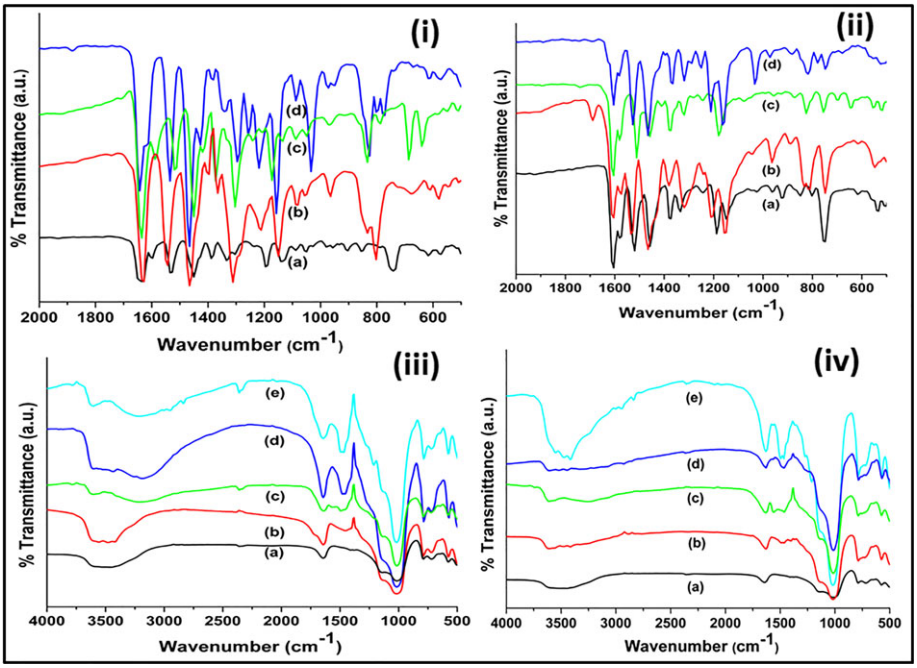

FIGURE 4 (i) FTIR spectra of free state salen complexes (a) CuS1, (b) CuS2, (c) CuS3 and (d) CuS4. (ii) FTIR spectra of free state salophen complexes (a) CuSp1, (b) CuSp2, (c) CuSp3 and (d) CuSp4. (iii) FTIR spectra of encapsulated copper salen complexes (a) pure zeolite Y, (b) CuS1-Y, (c) CuS2-Y, (d) CuS3-Y and (e) CuS4-Y. (iv) FTIR spectra of encapsulated copper salophen complexes (a) pure zeolite Y, (b) CuSp1-Y, (c) CuSp2-Y, (d) CuSp3-Y and (e) CuSp4-Y

to the presence of asymmetric stretching vibrations of (Si/Al)O_4 units of the framework. Other some prominent peaks are present at 560, 717, 786, 1643 and 3500 cm^{-1} position, which are mainly assigned to (Si/Al)O_4 bending mode, double ring, symmetric stretching vibrations, other two IR bands at 1643 and 3500 cm^{-1} positions are attributed to lattice water molecules and surface hydroxylic group.[6,31] These IR bands are remaining unaffected even after encapsulation processes. All the encapsulated complexes have exhibited the bands without any significant alternation in the peak positions, evidently revealing the fact that the host framework doesn't get modified during the complex formation inside the supercage. The suitable IR region for the characterization of encapsulated Schiff-base complex is 1200–1600 cm^{-1}, because in this region host lattice remains silent and observed IR peaks with smaller shifts are mainly due to the presence of guest complex within the framework having different environment from its free state. Studies in this region of 1200–1600 cm^{-1} become beneficial as some of the significant IR bands of the Schiff base complexes like C=N, C=C, C-O stretching and C-H deformation have emerged in this particular region, which are unaffected by host lattice. Comparative IR data indicates the complex formation in neat as well as in encapsulated state. Ligand (S1) has shown IR peaks at 1636 cm^{-1} and 1273 cm^{-1} which are assigned as C=N and C-O stretching, These IR bands are shifted towards lower wave numbers and appeared at 1634 cm^{-1} and 1194 cm^{-1} under complexation. In the encapsulated complexes these bands appear at comparative positions to free state complex and the higher shifts in $\nu_{C\text{-}H}$ deformation frequencies have already been attributed to the presence of complex inside the zeolite cavity.[32] The observed FTIR spectral data (Table S4) suggest the formation of copper Schiff-base complexes in the free and encapsulated states inside the zeolite Y supercage.

3.5 | X-ray photoelectron spectroscopy (XPS)

The existence of the guest metal complex in zeolite Y is also confirmed with the help of XPS study, which is an indirect technique to investigate the location of the metal complex in the host framework. The XPS survey spectra (given in supporting information Figure S6) and binding energy data of CuS1, CuS1-Y, and CuSp1-Y are presented in Table 3. It is observed that the elements/metal ions (C, N, O, Si, Al, and Cu^{2+}) are present in their respective surface chemical states in these complexes. The low concentration of metal contents in the encapsulated complexes makes the XPS signal for metal weak, which is actually in accordance with the concentration-dependent studies like IR, UV–Vis spectroscopy. The appearance of Cu(2p) peaks in XPS spectrum confirms the presence of copper

TABLE 3 Binding energy (eV) of free and encapsulated complexes

		Binding energy (eV)						
S. No	Samples	Si (2p)	Al (2p)	C (1 s)	N (1 s)	O (1 s)	Cu^{2+} (2p)	Δ2p
1	**CuS1**	-	-	283.35, 285.03	397.68, 399.61	531.26, 533.74	932.80, 952.72	19.92
2	**CuS1 -Y**	103.46	75.21	283.90, 285.76	397.65, 400.11	530.80, 533.08	934.13, 954.06	19.93
3	**CuSp1-Y**	103.56	75.23	284.13, 285.41	399.18 401.65	530.66, 532.88	934.17, 954.13	19.96

and is assigned to the Cu $2p_{3/2}$ and Cu $2p_{1/2}$ confirms the +2 oxidation state of Cu and square planar geometry of the complexes in the free and encapsulated states. Cu $2p_{3/2}$ and Cu $2p_{1/2}$ XPS signals have appeared at the binding energies of 932.80 eV and 952.72 eV respectively for the CuS1 complex whereas for the encapsulated complexes (CuS1-Y and CuSp1-Y) these peaks are slightly shifted towards the higher binding energies and have appeared at 934.13, 954.06 and 934.17, 954.13 eV respectively.[6,33] (XPS spectra presented in Figure 5) Such observed higher shifts in the binding energies upon encapsulation could be the result of lowering of electron density on the metal center because of the weakening in the delocalization of electrons due to alteration in the square planar proximity of the encapsulated complexes.[6] However, XPS signals for other atoms are more or less unshifted. C (1 s) signals in the free state CuS1 complex appear at 283.35 and 285.03 eV, which corresponds to the sp^2 and sp^3 carbon atoms respectively.[33] N (1 s) peaks for the complex are observed at binding energies 397.68 eV (M-N) and 399.61 eV (C=N) whereas O (1 s) peaks appear at the binding energies of 531.26 eV (M-O) and 533.74 eV (C-O).[23,33] These XPS peaks are observed at almost identical binding energies for the encapsulated complexes. For CuS1-Y-complex, the C(1 s) XPS signals are observed at 283.90, 285.76 eV and attributed to sp^2, sp^3 carbon atom whereas signals at 397.65, 400.11 eV and 530.80, 533.08 eV are attributed to (M-N, C=N) and (M-O, C-O) form of the respective elements. The equivalent XPS signals for CuSp1–Y complex are also observed at their corresponding binding energies; for the C (1 s), signals have appeared at 284.13, 285.41 eV, whereas N(1 s) and O (1 s) signals are observed at 399.18, 401.65 eV and 530.66, 532.88 eV respectively. Furthermore, both the encapsulated complexes have shown zeolitic Na(1 s), Al(2p) and Si(2p) XPS signals at their respective positions[6,23,33] (XPS spectra are presented in supporting information Figure S7-S9). Comparative XPS binding energy data of both free and encapsulated complexes, as well as higher shifts in binding energy for the Cu $2p_{3/2}$ and Cu $2p_{1/2}$ peaks in both encapsulated complexes, essentially signify the encapsulation of metal complexes inside the zeolite Y.

3.6 | DSC study

DSC curves recorded at a temperature range from 25 to 500 °C (heating rate: 10 °C/min and sample weight is taken: 3 mg) for zeolite-Y, CuS1 and CuS1-Y are shown in Figure 6. The neat copper complex CuS1 decomposes exothermically at a temperature range from 318 °C to 500 °C.[34] DSC curve of encapsulated copper complex CuS1-Y has shown a broad endothermic peak in between 30 to 300 °C which corresponds to the removal of water molecules adsorbed on zeolite surface.[35] Further heating leads to the appearance of two exothermic peaks in between 340 °C to 500 °C. Comparative studies with zeolite and neat complex indicate that these two peaks appeared for CuS1-Y are due to the decomposition of the encapsulated complex, as pure zeolite does not show any exothermic peak in that temperature range. The peaks are shifted towards higher temperatures compared to that of the neat complex signifying that the

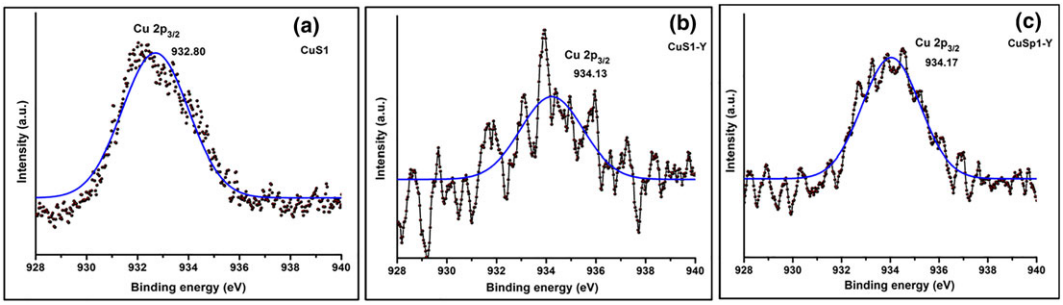

FIGURE 5 High resolution XPS spectra for the Cu $2p_{3/2}$ signal (a) CuS1, (b) CuS1-Y and (c) CuSp1- Y

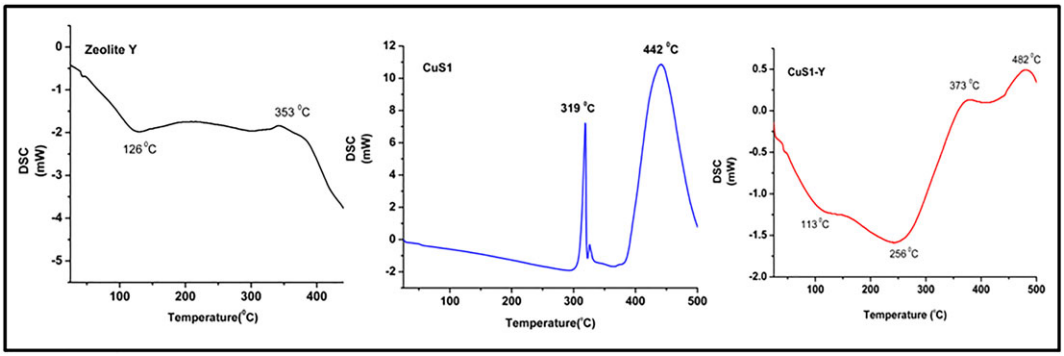

FIGURE 6 DSC curves of zeolite-Y, CuS1 and CuS1-Y

encapsulated metal complex is thermally more stable than the neat complex. A very small heat flow supports quite a low concentration of guest complex inside the supercage of zeolite-Y.

3.7 | TGA analysis

The TGA curves of pure zeolite Y, neat and encapsulated complexes are obtained in a nitrogen atmosphere and are shown in Figure 7 (TGA data given in Table 4). According to the TGA curve, weight loss for the neat copper complex CuS1 occurred in two steps. The first weight loss takes place in the temperature range (318–370)°C and in the second step, weight loss starts immediately after the first step in the range (371–560)°C suggesting decomposition of the chelating salen ligand.[22] For pure zeolite Y, weight loss (24%) is obtained in the one-step temperature range of (50–300)°C due to the loss of water molecules.[36] Unlike pure zeolite Y, the encapsulated copper complex CuS1-Y shows two-step weight losses. The first step weight loss occurs in the range of (50–300)°C corresponding to desorption of physically adsorbed water molecules from the zeolite framework with a mass loss of 11.6%. The second step involves the weight loss occurring after

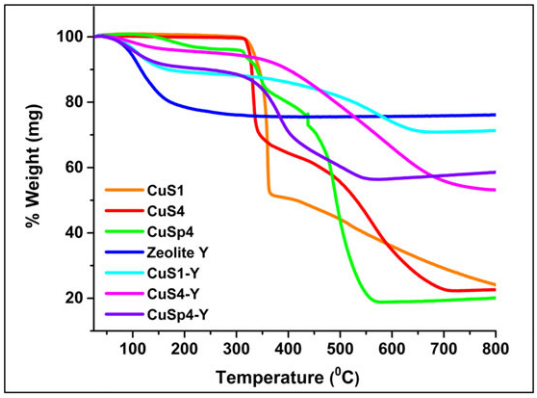

FIGURE 7 TGA curves of CuS1, CuS4, CuSp4, zeolite-Y, CuS1-Y, CuS4-Y and CuSp4-Y

TABLE 4 Thermogravimetric analysis data of free and encapsulated complexes

S.No.	Samples	Temperature range (°C)	Weight loss (%)
1	**Zeolite Y**	50–300	24.0
2	**CuS1**	318–370	48.5
		371–560	12.5
3	**CuS1-Y**	50–300	11.6
		340–660	16.5
4	**CuS4**	315–350	30.9
		351–700	46.1
5	**CuS4-Y**	50–300	5.5
		340–750	39.8
6	**CuSp4**	308–360	13.0
		361–575	64.8
7	**CuSp4-Y**	50–300	11.3
		320–580	31.1

340 °C with a mass loss of 16.5% which definitely corresponds to the loss of organic moieties from the zeolite cages.[36]

3.8 | BET surface area analysis

The BET surface area analysis has been performed to find out the surface area and pore volume of pure zeolite Y and encapsulated complexes. The comparative N_2 adsorption–desorption isotherms for zeolite Y and two of such encapsulated complexes (CuS4 and CuSp4 in zeolite) using BJH method are shown in Figure 8 along with the data of surface area and micropore volume, given in Table 5. The pattern of nitrogen sorption isotherms for all the catalysts are found to be nearly identical (Figure 8), indicating that the zeolite framework is not affected during the encapsulation process. All the catalysts have shown type I adsorption–desorption isotherms, which is a characteristic of the microporous material.[37] The lowering of BET surface areas and pore volumes of

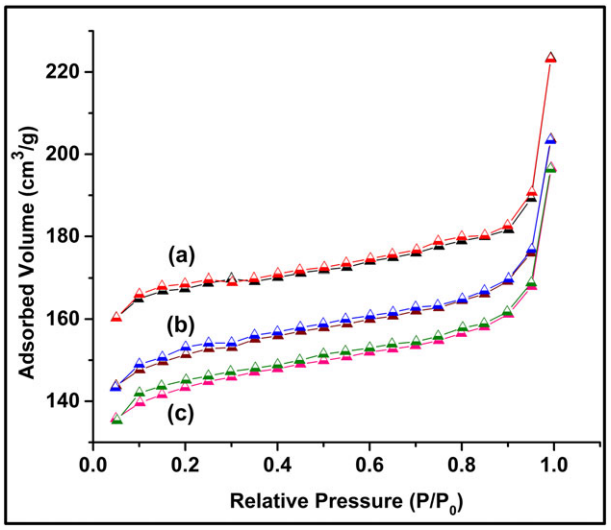

FIGURE 8 BET isotherms for pure zeolite-Y and zeolite encapsulated complexes: (a) pure zeolite Y, (b) CuS4-Y and (c) CuSp4-Y

TABLE 5 BET surface area and pore volume of pure zeolite Y, encapsulated complexes CuS4-Y and CuSp4-Y

S.No.	Sample	BET surface area (m^2/g)	Pore volume (cm^3/g)
1	Pure zeolite Y	535	0.3456
2	CuS4-Y	430	0.2735
3	CuSp4-Y	420	0.2611

both the zeolite samples with encapsulated copper complexes compared to that of pure zeolite Y clearly suggest the presence of metal complex within the supercage of zeolite Y rather than on the external surface.[19,22] The decreases in the surface area and pore volume of the catalyst largely depend upon the loading level of metal in zeolites along with the molecular dimension and geometry of the complex encapsulated inside the zeolite supercage.

3.9 | UV–visible study

To confirm the complex formation inside the cavity of zeolite and to study the co-ordination environment around the metal center, electronic spectroscopy is always being informative. The relative UV–Visible spectroscopic studies in the solid state of all the copper Schiff-base complexes presented in Figure 9 and Table 6 and solution UV–Visible spectra for CuS1 and CuSp3 are presented in supporting information Figure S10, thereby provide the significant evidence about the complex formation in both states. Absorption bands in the range of (230–250) nm are recognized as π-π^* transitions, whereas in the range of (300–384) nm are mainly assigned as n-π^* transitions. The electronic transitions, which are mainly originated from the metal d orbitals, are identified in the comparative lower energy region of the spectrum. Bands appeared in the range of (404–471) nm and (502–607) nm are attributed to charge transfer and d-d transitions respectively. UV–Visible data of free CuS1 complex have shown good concurrence with the reported data in the literature[38] and also provided the information about the complex formation in the free state. After the encapsulation in zeolite Y, complexes have shown a similar prototype of electronic spectra, indicating that the complexes are indeed present in the host lattice. Comparative studies of the electronic spectra of the complexes in free and their encapsulated states, make it quite clear that the intra-ligand transitions (π-π^* and n-π^*) are relatively unaffected under the encapsulation; however, transitions which are mainly instigated from the metal center are primarily altered in terms of peak positions as well as intensities for all guest complexes. It is quite interesting to perceive a regular blue shift and intensification of the d-d transitions in the encapsulated copper - Schiff-base complexes. Such behavior already has been observed in the zeolite Y encapsulated complexes.[23,28,32] Observed modified electronic behavior in the d-d region is certainly an effect of different geometry of the co-ordination sphere, which the guest complex has adopted under the space restrictions of host supercage. Theoretical studies have also revealed the fact that changes in the bond angles, bond lengths, and HOMO-LUMO gaps can be introduced in the guest complex by the process of encapsulation in zeolites.[28,31] In the present study, the copper complexes have chosen on the basis of their molecular dimensions (i.e., end to end distances) of the complexes, which follow the order as CuS1 < CuS2 < CuS3 < CuS4 and CuSp1 < CuSp2 < CuSp3 < CuSp4 for the salen and salophen copper complexes respectively. The complex with larger molecular dimensions experiences the more steric impulsion and obviously, it adopts more distorted geometry to accommodate itself into the framework cavity. There are some interesting reports, which have explored the correlation between the geometry of the metal complexes and different factors and their consequence. It is previously studied that effect of the substituent groups (-Cl and $-OCH_3$) on the geometry of copper Schiff-base complexes is so prominent.[2,39] Another report has revealed that the replacement of the atoms in the N_2O_2 square planar proximity by N_2OS and N_2S_2 leads the distortion in the geometry of that complex and its effect can be seen in the optical behavior of that complex.[40] Sankar *et al.* have suggested that the different substituent groups can cause the push-pull effect on the

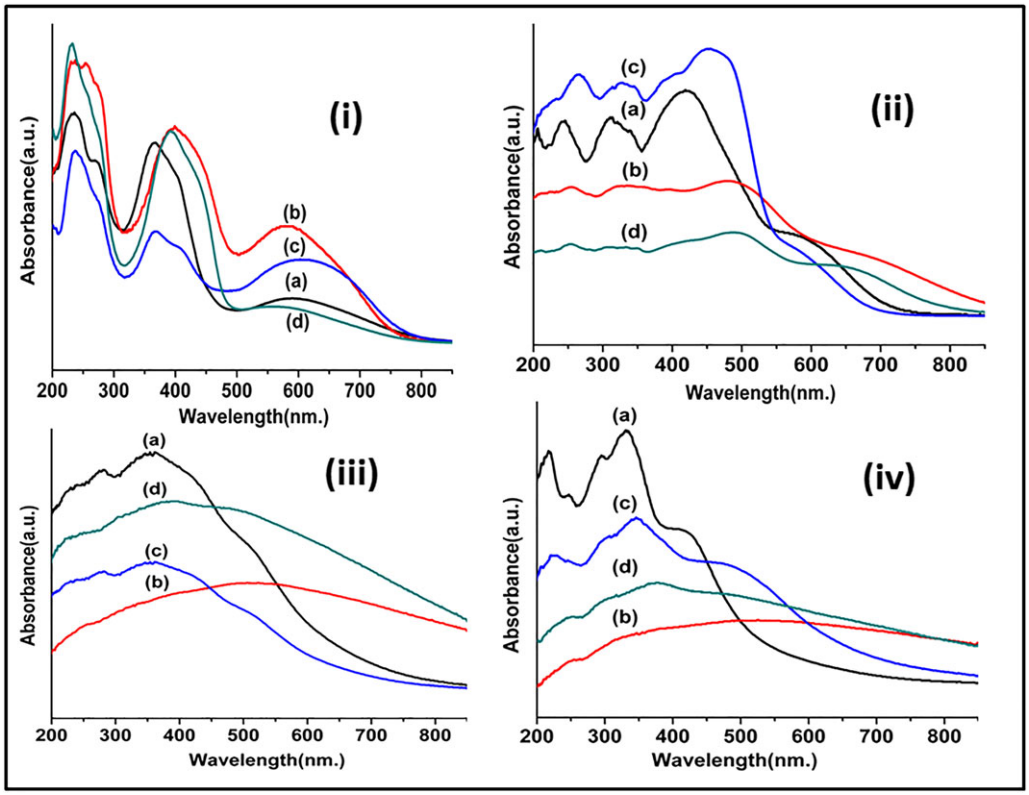

FIGURE 9 (i) Solid state UV-Vis spectra of free satate copper salen complex (a) CuS1, (b) CuS2, (c) CuS3 and (d) CuS4. (ii) The solid state UV-Vis spectra of free state copper salophen complex (a) CuSp1, (b) CuSp2, (c) CuSp3 and (d) CuSp4. (iii) The solid state UV-Vis spectra of encapsulated copper salen complexes in zeolite Y (a) CuS1-Y, (b) CuS2-Y, (c) CuS3-Y and (d) CuS4-Y. (iv) The solid state UV-Vis spectra of encapsulated copper salophen complexes in zeolite Y, (a) CuSp1-Y, (b) CuSp2-Y, (c) CuSp3-Y and (d) CuSp 4-Y

TABLE 6 Solid state UV–Visible spectroscopic data of complexes in free and encapsulated state

S.No	Samples	π—π^* transitions	n—π^* transitions	CT transitions	d-d transitions
1	**CuS1**	232	364	404	592
2	**CuS1-Y**	234	362	417	533
3	**CuS2**	248	397	447	584
4	**CuS2-Y**	252	395	471	514
5	**CuS3**	238	367	406	609
6	**CuS3-Y**	232	360	419	528
7	**CuS4**	232	391	435	592
8	**CuS4-Y**	241	387	418	495
9	**CuSp1**	246	306	419	607
10	**CuSp1-Y**	249	300	423	588
11	**CuSp2**	251	347	479	668
12	**CuSp2-Y**	253	343	394	567
13	**CuSp3**	249	336	445	502
14	**CuSp3-Y**	247	338	471	610
15	**CuSp4**	253	321	484	646
16	**CuSp4-Y**	251	315	382	503

porphyrin complexes which is actually associated with the change in the energy gaps in the d-d orbitals.[41] In the present study we have observed a nice correlation between the observed blue shift in d-d bands and the molecular dimensions of the copper Schiff base complexes. On encapsulation, the complexes with largest molecular dimension in both the series (CuS4 and CuSp4) are expected to adopt the most distorted geometries, which are actually depicted as maximum blue shifted d-d bands in the electronic spectrum, whereas CuS1 and CuSp1 complexes have shown minimum blue shifts. The degree of blue shift in d-d bands is just in accordance to the increasing order of the molecular dimensions of complexes and the order is CuS1 < CuS2 < CuS3 < CuS4 and CuSp1 < CuSp2 < CuSp3 < CuSp4 for the salen and salophen complexes respectively. This behavior of complexes is quite reasonable and can be well-correlated with the extent of distortion and molecular dimensions of the guest complex and their consequence in the optical spectra.

3.10 | Structural and functional correlations

It is quite interesting to note that the reactivity in terms of turn over number (TON) of encapsulated complexes is substantially higher compared to the corresponding free state complexes. These observations signify that encapsulation within the supercage of zeolite has converted the metal complexes significantly reactive and hence, to achieve the same extent of activity, required active catalytic sites are much lesser in quantity. This makes the zeolite-encapsulated complexes as attractive heterogeneous catalysts for various organic oxidative transformations.[29,31] The modified reactivity of the encapsulated complexes is mostly a consequence of the distorted geometry of the complexes they adopt, under encapsulation in zeolite Y. Copper Schiff-base complexes are generally efficient catalysts in solution as well as heterogeneous phases in comparisons to their corresponding nickel analogues. Crystal study of these complexes evidently indicates that copper metal is out of the square CuN_2O_2 proximity and shows distorted square planar geometry, whereas nickel Schiff base complexes are slightly less distorted retaining its nearly square planar geometry.[42] These complexes when encapsulated in zeolite Y, are further distorted due to space constraint imposed by rigid host zeolite supercage. As a consequence, depletion in the electron density on the metal center takes place. Comparative shifts towards the higher value of binding energy in XPS signals for the zeolite-encapsulated complexes also support the generation of more electropositive metal center in encapsulated complexes. Encapsulation, therefore, appears to be an effective alternative approach to generate more electron deficient metal center in guest complex inside the rigid zeolite host.[2] Lower the electron density on the metal center, more receptive the metal center is for the nucleophilic attack. However, the depletion of electron density can also be achieved by an addition of electron withdrawing group (-Cl).[43] It has been also discussed that an electron withdrawing (-Cl) substituent makes the complex essentially monomer in solid state with distorted square-planar geometry around the metal. The report states that distorted chloro - copper salen complex provides the admixing of the ground state d_{xy} orbital with d_z^2 orbital and thereby enhances the stability of electron-rich axial ligand complex suggesting that electron withdrawing group on the phenyl rings makes the metal complex significantly non-planar. However, an electron donating group ($-OCH_3$) on the same position maintains the planarity of the complex. Planar conjugated system makes the metal center rich with electron density so that it acts as a less efficient receptive center for the nucleophilic attacks. Recently, it is observed experimentally as well as theoretically that the nickel (II) Schiff-base complexes with different molecular dimensions adopt distorted geometry under encapsulation in zeolite Y. Largest complex experiences more distortion and shows the most enhanced catalytic activity for styrene oxidation after the encapsulation. Interestingly, this complex is least reactive for the same catalytic process in its free state.[23] In the present study, the parallel behavior of zeolite Y encapsulated copper salen complexes is observed for the oxidation of styrene in presence of H_2O_2. Detailed catalytic studies for the series of salen complexes have indicated that the CuS3 complex is the most reactive for the styrene oxidation in a free state. Electron withdrawing -Br group in CuS3 makes the complex distorted even in its free state. As a consequence, the complex is more reactive towards the nucleophillic attack stabilizing the electron-rich axial ligand (nucleophile) in the transition state (proposed mechanism for styrene oxidation is presented in supporting information Figure S11). In the other series, CuSp3 complex shows slightly lesser reactivity than expected, the reason could be the low solubility of the complex in the reaction medium. Encapsulation of CuS3 and CuSp3 complexes inside the supercage further enhances the degree of distortion and makes the metal, even more, electron deficient and consequently more reactive. The performance of the catalysts is well understood, as the main decisive factors like an electronic factor of electron withdrawing groups and space constraint imposed by zeolite Y under encapsulation are additive

to each other and working in synergistic fashion here. Free state CuS2, CuSp2, CuS4, and CuSp4 complexes are not as much reactive, since they may exist in the dimeric form in their solution states,[39] or because of the less receptive copper metal center for the nucleophillic attack of H_2O_2 since all these complexes have electron donating groups attached on the phenyl rings. However, these complexes when encapsulated in zeolite Y, have shown very exciting catalytic behavior. Among all, the most striking observation is with CuS4 and CuSp4 complexes as when encapsulated they have shown remarkable enhancement in reactivity for the above-mentioned reaction. On encapsulation, TON of CuS4 catalyst increases from 650 to 3137 and that of CuSp4 enhances even remarkably from 187 to 3543. Hence the competence of these heterogeneous systems is mainly driven by the electron deficiency of the metals administered by the steric factor, which actually opposes the original electronic factor of substituent groups (-OCH_3). The electron deficient character of the metals via steric constraint imposed by the topology of zeolite supercage dominates and enhances the reactivity as the addition of two -OCH_3 groups on phenyl rings makes the complex largest in the series and hence more distorted inside the rigid host cavity of zeolite Y. Consequently, the metal center becomes more electropositive, showing extraordinarily higher catalytic activities. CuS2 and CuSp2 complexes having electron donating substituent groups (-OH) and with moderate molecular dimensions when encapsulated, are not so efficient catalysts as CuS4, and CuSp4 complexes in their encapsulated states. For CuS2, inherent electronic factor and electronic factor is driven by steric constraints oppose each other and eventually their contributions become comparable as indicated by TON (shown in Table 2) after encapsulation in zeolite Y. However, being larger than CuS2, encapsulated CuSp2 complex shows enhancement of catalytic activity as steric constraints obscure the inherent electron effect. Overall catalytic data have illustrated the reactivity of free state copper Schiff-base complexes driven by only the electronic factor and therefore the trend of reactivity follows the order as CuS3 > CuS1 > CuS2 > CuS4 for salen and CuSp1 > CuSp3 > CuSp2 > CuSp4 for salophen complexes. After encapsulation of complexes in the zeolite Y, the reactivity order is mainly driven by molecular dimensions and extent of distortion of the guest complexes. The catalytic reactivity order in the encapsulated state for the salen complexes therefore becomes CuS4 > CuS3 > CuS1 > CuS2, whereas the salophen complexes demonstrate the following order: CuSp4 > CuSp3 > CuSp2 > CuSp1. The experimentally observed blue shift of d-d transition in electronic spectra also support above catalytic order of the encapsulated complexes; larger is the blue shift, more will be the catalytic activity. A further interesting observation, while comparing the catalytic activities of salen with that of salophen complexes in both states, is the reactivity of copper salen and salophen complexes are approximately comparable, however, that is not the case for encapsulated analogues. Only CuS1 and CuSp1 complexes show comparable reactivity however other substituted copper salophen complexes are definitely better catalysts than the corresponding salen complexes. Larger is the molecular dimensions of a complex, more is the reactivity after the encapsulation in the zeolite Y towards the styrene oxidation reaction.

4 | CONCLUSION

Zeolite framework certainly provides a route to design the heterogeneous catalyst with customized reactivity by the encapsulation process. Rigid walls of framework impose space restraint on the guest complex forcing the guest complex to adopt distorted structure. Such alteration in the structure of the complex plays a crucial role for the modified reactivity of the system. The observed blue shift in a d-d band in electronic spectra signifies the alternation in the metal d orbitals energy levels, which is certainly an effect of the altered coordination sphere around the metal center. This adaptation of nearly planar geometry finally leads to the non-planar geometry and as a consequence, metal center becomes more electropositive. Non-planar geometry impedes the conjugation around the metal center. XPS studies also support the enhanced electropositive character of the metal in the encapsulated complexes as the $Cu_{2p/3}$ (II) XPS signal for the encapsulated complexes shifts towards higher binding energy. More electropositive character of the metal center, more susceptible it will be for the nucleophilic attack of H_2O_2. It is quite obvious that the larger molecular dimension leads more deformation in the geometry of the complex and as a consequence, more active metal center is created in the encapsulated state of the complex. Comparative catalytic studies of these hybrid systems provide a fascinating correlation between modified structural aspects and modified functionality of complexes, and therefore it can be concluded, as the degree of distortion in the structure of the encapsulated complex is the key point for the remarkable modified catalytic activity of the systems.

ACKNOWLEDGEMENTS

The authors acknowledge the DST, New Delhi, for the financial support (DST Project no. SR/FT/CS-038/2010)

and for the instrumental facility funded by DST-FIST, Department of Chemistry and Department of Physics, BITS, Pilani, for the XPS measurement, and MNIT Jaipur.

ORCID

Saumi Ray https://orcid.org/0000-0002-6893-9634

REFERENCES

[1] a) N. Y. Chen, W. E. Garwood, *J. Catal.* **1978**, *52*, 453. b) J. R. Anderson, K. Foger, T. Mole, R. A. Rajadhyaksha, J. V. Sanders, *J. Catal.* **1979**, *58*, 114.

[2] S. Deshpande, D. Srinivas, P. Ratnasamy, *J. Catal.* **1999**, *188*, 261.

[3] M. R. Maurya, A. K. Chandrakar, S. Chand, *J. Mol. Catal. A Chem.* **2007**, *274*, 192.

[4] a) C. Jin, W. Fan, Y. Jia, B. Fan, J. Ma, R. Li, *J. Mol. Catal. A Chem.* **2006**, *249*, 23. b) E. R. Shilpa, V. Gayathri, *J. Environ. Chem. Eng.* **2016**, *4*, 4194. c) M. Salavati-Niasari, *J. Mol. Catal. A Chem.* **2005**, *229*, 159. d) M. Salavati-Niasari, A. Sobhani, *J. Mol. Catal. A Chem.* **2008**, *285*, 58. e) M. Salavati-Niasari, *J. Mol. Catal. A Chem.* **2008**, *283*, 120. f) M. Salavati-Niasari, F. Davar, *Inorg. Chem. Commun.* **2006**, *9*, 263.

[5] K. J. Balkus, A. G. Gabrielov, in *Inclusion Chemistry with Zeolites: Nanoscale Materials by Design*, (Eds: N. Herron, D. R. Corbin), Springer Netherlands, Dordrecht **1995** 159.

[6] K. K. Bania, R. C. Deka, *J. Phys. Chem. C* **2013**, *117*, 11663.

[7] a) J. Zhu, Z. Kónya, V. F. Puntes, I. Kiricsi, C. X. Miao, J. W. Ager, A. P. Alivisatos, G. A. Somorjai, *Langmuir* **2003**, *19*, 4396. b) D. E. De Vos, M. Dams, B. F. Sels, P. A. Jacobs, *Chem. Rev.* **2002**, *102*, 3615.

[8] a) C.-Y. Sun, X.-L. Wang, X. Zhang, C. Qin, P. Li, Z.-M. Su, D.-X. Zhu, G.-G. Shan, K.-Z. Shao, H. Wu, J. Li, *Nat. Commun.* **2013**, *4*, 2717. b) P. Ling, J. Lei, L. Zhang, H. Ju, *Anal. Chem.* **2015**, *87*, 3957.

[9] D. T. Genna, A. G. Wong-Foy, A. J. Matzger, M. S. Sanford, *J. Am. Chem. Soc.* **2013**, *135*, 10586.

[10] a) Q. Yao, Y. Zhang, *Angew. Chem. Int. Ed. Engl.* **2003**, *42*, 3395. b) I. J. B. Lin, C. S. Vasam, *J. Organomet. Chem.* **2005**, *690*, 3498.

[11] M. Benjamin, D. Manoj, K. Thenmozhi, P. R. Bhagat, D. Saravanakumar, S. Senthilkumar, *Biosens. Bioelectron.* **2017**, *91*, 380.

[12] M. Salavati-Niasari, P. Salemi, F. Davar, *J. Mol. Catal. A Chem.* **2005**, *238*, 215.

[13] a) M. Cinouini, S. Colonna, H. Molinari, F. Montanari, P. Tundo, *J. Chem. Soc. Chem. Commun.* **1976**, *394*. b) X. Zuwei, Z. Ning, S. Yu, L. Kunlan, *Science* **2001**, *292*, 1139.

[14] M. R. Maurya, A. K. Chandrakar, S. Chand, *J. Mol. Catal. A Chem.* **2007**, *263*, 227.

[15] a) C. Bowers, P. K. Dutta, *J. Catal.* **1990**, *122*, 271. b) A. A. Valente, J. Vital, in Studies in Surface Science and Catalysis, *Vol. 108*, (Eds: H. U. Blaser, A. Baiker, R. Prins), Elsevier **1997** 461. c) M. Salavati-Niasari, *Microporous Mesoporous Mater.* **2006**, *95*, 248. d) M. Salavati-Niasari, *Inorg. Chem. Commun.* **2006**, *9*, 628. e) M. Salavati-Niasari, M. Bazarganipour, *Catal. Commun.* **2006**, *7*, 336. f) M. Salavati-Niasari, E. Zamani, M. R. Ganjali, P. Norouzi, *J. Mol. Catal. A: Chem.* **2007**, *261*, 196.

[16] a) F. Bedioui, *Coord. Chem. Rev.* **1995**, *144*, 39. b) S.-N. Masoud, *Chem. Lett.* **2005**, *34*, 1444. c) M. Salavati-Niasari, *Inorg. Chem. Commun.* **2005**, *8*, 174. d) S.-N. Masoud, *Chem. Lett.* **2005**, *34*, 244. e) M. Salavati-Niasari, *Inorg. Chem. Commun.* **2004**, *7*, 963. f) M. Salavati-Niasari, *Polyhedron* **2009**, *28*, 2321.

[17] R. F. Parton, I. F. J. Vankelecom, M. J. A. Casselman, C. P. Bezoukhanova, J. B. Uytterhoeven, P. A. Jacobs, *Nature* **1994**, *370*, 541.

[18] a) M. R. Maurya, A. K. Chandrakar, S. Chand, *J. Mol. Catal. A Chem.* **2007**, *270*, 225. b) B. Neelam, N. Fehmida, B. Alok, B. Sudha, A. Amir, *Eur. J. Med. Chem.* **2000**, *35*, 481. c) M. Maurya, S. Titinchi, S. Chand, I. Mishra, *J. Mol. Catal. A Chem.* **2002**, *180*, 201. d) M. R. Maurya, S. J. Titinchi, S. Chand, *J. Mol. Catal. A Chem.* **2003**, *201*, 119.

[19] D. R. Godhani, H. D. Nakum, D. K. Parmar, J. P. Mehta, N. C. Desai, *J. Mol. Catal. A Chem.* **2017**, *426*, 223.

[20] a) M. Martis, K. Mori, H. Yamashita, *Dalton Trans.* **2014**, *43*, 1132. b) S. Seelan, A. K. Sinha, *Appl. Catal., A* **2003**, *238*, 201.

[21] S. Bhar, R. Ananthakrishnan, *Photochem. Photobiol. Sci.* **2017**, *16*, 1290.

[22] M. Sharma, B. Das, G. V. Karunakar, L. Satyanarayana, K. K. Bania, *J. Phys. Chem. C* **2016**, *120*, 13563.

[23] A. Choudhary, B. Das, S. Ray, *Dalton Trans.* **2016**, *45*, 18967.

[24] M. Salavati-Niasari, Z. Salimi, M. Bazarganipour, F. Davar, *Inorg. Chim. Acta* **2009**, *362*, 3715.

[25] M. M. Bhadbhade, D. Srinivas, *Inorg. Chem.* **1993**, *32*, 6122.

[26] a) K. O. Xavier, J. Chacko, K. K. Mohammed Yusuff, *Appl. Catal. A Gen.* **2004**, *258*, 251. b) S. Sharma, S. Sinha, S. Chand, *Ind. Eng. Chem. Res.* **2012**, *51*, 8806. c) C. R. Jacob, S. P. Varkey, P. Ratnasamy, *Appl. Catal. A Gen.* **1998**, *168*, 353. d) G. Ramanjaneya Reddy, S. Balasubramanian, K. Chennakesavulu, *J. Mater. Chem. A* **2014**, *2*, 15598. e) G. R. Reddy, S. Balasubramanian, K. Chennakesavulu, *J. Mater. Chem. A* **2014**, *2*, 19102. f) M. R. Maurya, A. K. Chandrakar, S. Chand, *J. Mol. Catal. A Chem.* **2007**, *263*, 227. g) M. R. Maurya, A. K. Chandrakar, S. Chand, *J. Mol. Catal. A: Chem.* **2007**, *274*, 192.

[27] J. Deka, L. Satyanarayana, G. V. Karunakar, P. K. Bhattacharyya, K. K. Bania, *Dalton Trans.* **2015**, *44*, 20949.

[28] A. Choudhary, B. Das, S. Ray, *Dalton Trans.* **2015**, *44*, 3753.

[29] M. R. Maurya, B. Singh, P. Adão, F. Avecilla, J. Costa Pessoa, *Eur. J. Inorg. Chem.* **2007**, *2007*, 5720.

[30] W. H. Quayle, G. Peeters, G. L. De Roy, E. F. Vansant, J. H. Lunsford, *Inorg. Chem.* **1982**, *21*, 2226.

[31] K. K. Bania, D. Bharali, B. Viswanathan, R. C. Deka, *Inorg. Chem.* **2012**, *51*, 1657.

[32] R. Ganesan, B. Viswanathan, *J. Phys. Chem. B* **2004**, *108*, 7102.

[33] G. Ramanjaneya Reddy, S. Balasubramanian, K. Chennakesavulu, *J. Mater. Chem. A* **2014**, *2*, 15598.

[34] a) Y. Yang, H. Ding, S. Hao, Y. Zhang, Q. Kan, *Appl. Organomet. Chem.* **2011**, *25*, 262. b) B. Cristóvão, J. Kłak, B. Miroslaw, *J. Coord. Chem.* **2014**, *67*, 2728. c) É. T. G. Cavalheiro, F. C. D. Lemos, J. Z. Schpector, E. R. Dockal, *Thermochim. Acta* **2001**, *370*, 129.

[35] L. Wu, A. Navrotsky, *Phys. Chem. Chem. Phys.* **2016**, *18*, 10116.

[36] S. L. Hailu, B. U. Nair, M. Redi-Abshiro, I. Diaz, R. Aravindhan, M. Tessema, *Chin. J. Catal.* **2016**, *37*, 135.

[37] B. Kumar Kundu, V. Chhabra, N. Malviya, R. Ganguly, G. S. Mishra, S. Mukhopadhyay, *Microporous Mesoporous Mater.* **2018**, *271*, 100.

[38] S. Koner, *Chem. Commun.* **1998**, *593*.

[39] M. M. Bhadbhade, D. Srinivas, *Inorg. Chem.* **1993**, *32*, 6122.

[40] L. Gomes, E. Pereira, B. de Castro, *J. Chem. Soc. Dalton Trans.* **2000**, *1373*.

[41] N. Grover, M. Sankar, Y. Song, K. M. Kadish, *Inorg. Chem.* **2016**, *55*, 584.

[42] A. Boettcher, H. Elias, E. G. Jaeger, H. Langfelderova, M. Mazur, L. Mueller, H. Paulus, P. Pelikan, M. Rudolph, M. Valko, *Inorg. Chem.* **1993**, *32*, 4131.

[43] M. M. Bhadbhade, D. Srinivas, *Inorg. Chem.* **1993**, *32*, 6122.

SUPPORTING INFORMATION

Additional supporting information may be found online in the Supporting Information section at the end of the article.

How to cite this article: Kumari S, Choudhary A, Ray S. The functionality of the hybrid systems driven by molecular dimension of the guest copper Schiff-base complexes entrapped in Zeolite-Y. *Appl Organometal Chem*. 2019;e4765. https://doi.org/10.1002/aoc.4765